IOP Conference Series: Earth and Environmental Science

Identification of the precessing vortex core in a hydro turbine model using local stability analysis and stochastic modeling

To cite this article: Ivan Litvinov *et al* 2022 *IOP Conf. Ser.: Earth Environ. Sci.* **1079** 012052

IOP Conf. Series: Earth and Environmental Science 1079 (2022) 012052 doi:10.1088/1755-1315/1079/1/012052

Identification of the precessing vortex core in a hydro turbine model using local stability analysis and stochastic modeling

Ivan Litvinov[1,2], Moritz Sieber[3], and Kilian Oberleithner[3]

[1] Kutateladze Institute of Thermophysics SB RAS, Russia
[2] Novosibirsk State University, Russia
[3] Technische Universität Berlin, Germany

E-mail: `litvinov@itp.nsc.ru`

Abstract. Stochastic modeling and local linear stability analysis (LSA) is employed to predict the onset of the precessing vortex core (PVC) in the hydro turbine model. The method of the stochastic modeling based on the pressure fluctuation signals correctly predicts the instability of the azimuthal mode $m = 1$ at flow rates below $0.7Q_c$. This is in line with local LSA that shows that the azimuthal modes $m = 1$ and $m = 2$ are absolutely unstable below the flow rate of $0.7Q_c$. The absolute instability of mode $m = 2$ is a new observation in the part load regimes of hydro turbines and plays a significant role in the dynamics of the PVC. As demonstrated in this paper, local LSA and stochastic modelling are both methods to uncover the driver of the PVC using sparse experimental data stemming from either spatially resolved but non-timeresolved PIV snapshots or single-point time-resolved wall pressure recordings, respectively. This makes these methods suitable to be applied to configurations of industrial relevance.

1. Introduction

Hydropower is a well suited energy source for balancing energy contributions for another renewable sources due to flexible operation capabilities. This fact encourages hydro turbines to operate at off-design conditions. At part load operating conditions, a strong swirl flow is generated in the draft tube that gives rise to vortex breakdown in the form of helical structure [1]. It is well known as the precessing vortex core (PVC) or the vortex rope appears in combustion systems [2] and in a hydro turbine water path [3].

The physical mechanism responsible for the PVC occurrence is the key to the flow control of the PVC and further extending the operating range of the hydro turbine. The stochastic modeling (SM) and the local linear stability analysis (LSA) are well suited analytic frameworks to meet this issue. The SM framework is based on deterministic behaviour of the global mode (PVC) and the perturbations by the background turbulence. The robust applications of the SM approach are given for the swirl model combustors [4, 5]. The main advantage of the SM method is accurate prediction of PVC formation in the flow for the critical parameters of the flow based only on the point pressure measurements.

The LSA is one of the promising instruments to predict PVC formation in the swirl flow. From the LSA approach point of view, the PVC is interpreted as a global mode of the mean flow [6]. The local LSA is based on a parallel-flow assumptions, which has the advantage that boundary conditions do not need to be specified in upstream and downstream direction. This is preferable when dealing with limited experimental data [6, 7]. The LSA is a well-proven framework and widely used in different swirl flows.

In this work, we show results of the SM approach based on the data of pressure fluctuations, and the critical swirl number in terms of PVC formation in the flow is predicted. Also, we conduct the local LSA to predict the PVC formations based on the mean velocity fields taken from PIV measurements reported in [8]. The local LSA shows that azimuthal modes $m = 1$ and $m = 2$ are absolutely unstable for part-load regimes of the hydro turbine (flow rates $0.3-0.7Q_c$). It provides new insight on the results presented in [8], where the impact of mode $m = 2$ to the energy content is observed to be significant in the part load regimes $0.5 - 0.55Q_c$.

2. Methods

2.1. Experimental method

The air experimental rig is described in details in the works [8, 9]. Figure 1 shows the sketch of the test section of the rig. The pair of swirlers generates the velocity distribution to model real hydro turbine distribution of velocity. The swirlers designed for the Best Efficiency Point (BEP) of the Francis turbine [10]. This BEP regime corresponds to a flow rate of $Q_c = 174.6$ m^3/h and a clockwise rotating runner speed of $n_c = 40.5$ Hz. After passing through the swirler system, the flow goes to the Francis-99 draft tube. The diameter of the draft tube inlet D is 100 mm. The flow is studied for the operating parameters of the flow rate in the range from $0.3Q_c$ to $0.8Q_c$ to cover part load operation conditions. Figure 1 shows the PIV domain and the

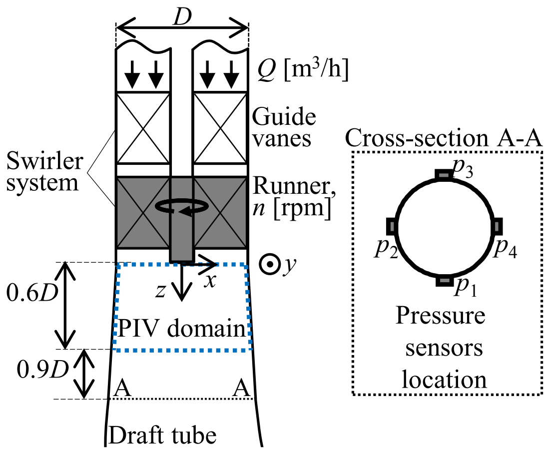

Figure 1. Experimental air set-up.

region of pressure pulsation measurements. The low-repetition-rate PIV system is used (1 Hz). Details of the PIV system can be found in the work [8]. For each operating regime, statistics of 1500 snapshots are collected.

The four Behringer ECM8000 microphones mounted at the opposite four azimuthal positions are used to record the pressure fluctuations on the cone walls in the cross-section A-A as shown in Figure 1. For each operating condition, pressure fluctuation signals are digitized (sampling rate of 20 kHz). For the SM approach, we have used the pressure fluctuation recordings with a good statistics in time to obtain the PVC amplitude. The length of each signal is 900 seconds. The pressure recordings of p_n are decomposed into spatial Fourier modes according to [5]. Then, each signal corresponds to azimuthal mode m as

$$\hat{p}_m(t) = \frac{1}{4}\sum_{n=1}^{4} p_n e^{-imn2\pi/4}. \tag{1}$$

The PVC is characterized by first azimuthal mode $A = \hat{p}_1$, which corresponds to a single helical vortex structure. To improve the quality of the signals, $A = \hat{p}_1$ we have used a band-pass filter with the band $[\frac{2}{3}f_{PVC}, \frac{3}{2}f_{PVC}]$.

2.2. Stochastic modeling

A detailed description of the SM approach is presented for the swirl model combustors in [4, 5]. The analysis focuses on the signal of pressure fluctuation $A(t)$ (described in section 2.1) to obtain reliable parameters of the SM model.

The Stuart-Landau equation describes the oscillatory motion of the global mode and the corrections of the mean field, which lead to amplitude saturation into limit-cycle. According to [4, 5], the PVC is also a consequence of a global mode. Then, the Stuart-Landau equation is well suited to describe the PVC dynamics in terms of complex amplitude of the global mode A: [5]:

$$\frac{dA}{dt} = (\sigma + i\omega)A - \alpha|A|^2 A + \xi. \tag{2}$$

It follows, that the amplitude depends on such parameters as the frequency ω, the amplification rate σ, and the saturation α. In our analysis, we have interested in the amplification rate σ due to negative values ($\sigma < 0$) refer to a stable system and positive values ($\sigma > 0$) to an unstable system.

The next step of the SM approach is to find the evolution of flow regime in the form of probability density function (PDF) of the pressure fluctuations amplitude, which could be described by Fokker-Planck equation:

$$P(|A|) = Nexp(\frac{2\sigma}{\Gamma}|A|^2 - \frac{\alpha}{\Gamma}|A|^4), \tag{3}$$

where the unknown parameters could be found by calibration with the measured PDF $P_{exp}(|A|)$, where N is a normalizing constant. To fit the model to experimental PDF $P_{exp}|A|$, the optimization of the Kulback-Leibler divergence is used. The effective noise intensity Γ defines as

$$\Gamma = \frac{4\tau D_\xi}{\tau^2\omega^2 + 1}, \tag{4}$$

where the noise parameter D_ξ is related to the variance of phase distortion $\xi_\phi = |A|(\dot{\phi} - 2\pi f_{PVC})$ and τ is the noise timescale. In this work, we identified the noise timescale to be approximately $\tau = 100/f_s$, where f_s is the sample frequency. According to previous investigation [5], it is correct, if the parameter τ is smaller than the $1/\omega$.

2.3. Linear stability analysis

According to [11], velocity vector $\mathbf{v}(\mathbf{x}, t)$ can be decomposed as

$$\mathbf{v}(\mathbf{x}, t) = \mathbf{V}(\mathbf{x}) + \tilde{\mathbf{v}}(\mathbf{x}, t) + \mathbf{v}''(\mathbf{x}, t), \tag{5}$$

where $\mathbf{V}(\mathbf{x})$ is the mean contribution, $\tilde{\mathbf{v}}$ is the periodic wave, and $\mathbf{v}''(\mathbf{x}, t)$ corresponds to the turbulent motion.

The substituting of the triple decomposition into the Navier-Stokes Equations results in three parts. The equations of the mean flow indicate the impact of the generation of the turbulent and coherent Reynolds stresses on the mean field

$$\begin{aligned} \bar{\mathbf{v}} \cdot \nabla \bar{\mathbf{v}} = -(1/\rho)\nabla \bar{p} + (1/Re)\nabla^2 \bar{\mathbf{v}} - \nabla \cdot (\overline{\mathbf{v}''\mathbf{v}''} + \overline{\tilde{\mathbf{v}}\tilde{\mathbf{v}}}), \\ \nabla \cdot \bar{\mathbf{v}} = 0, \end{aligned} \tag{6}$$

The equations of the periodic wave reads as follows

$$\begin{aligned} \frac{\partial \tilde{\mathbf{v}}}{\partial t} + \tilde{\mathbf{v}} \cdot \nabla \bar{\mathbf{v}} + \bar{\mathbf{v}} \cdot \nabla \tilde{\mathbf{v}} = -(1/\rho)\nabla \tilde{p} + (1/Re)\nabla^2 \tilde{\mathbf{v}} - \nabla \cdot (\tau^N - \tilde{\tau}) \\ \nabla \cdot \tilde{\mathbf{v}} = 0. \end{aligned} \tag{7}$$

The nonlinear terms τ^N can be neglected, and the unknown term $\tilde{\tau} = \widetilde{\mathbf{v}''\mathbf{v}''}$ represents the turbulent-coherent interactions. It can be modelled with a Boussinesq approximation,

$$\widetilde{\mathbf{v}''\mathbf{v}''} = -\nu_t(\nabla + \nabla^\top) \cdot \tilde{\mathbf{v}}. \tag{8}$$

It follows that, only one unknown parameter, called eddy viscosity ν_t, should be determined. For the instant, Rukes et al. [12] researched different eddy viscosity estimations to use it in the linear stability analysis. We will follow a more simplified and robust form of eddy viscosity model based on turbulent kinetic energy (TKE, k). According to [13], the eddy viscosity is estimated as

$$\nu_t = c l_m \sqrt{k}, \tag{9}$$

where the empirical constant is defined as $c = 0.55$ and the parameter l_m is called the turbulent mixing length. It represents the value of the size of the coherent structure in the flow, which could be estimated as $l_m = c_{\text{prop}} l$, where the empirical constant is defined as $c_{\text{prop}} = 0.075$, based on [14].

To estimate the typical size of the coherent structure in the flow, the distance between the maximum and the minimum of mean axial velocity is used. This value is shown in the Figure 2a. The length l slightly increase with increasing of axial coordinates (Figure 2b).

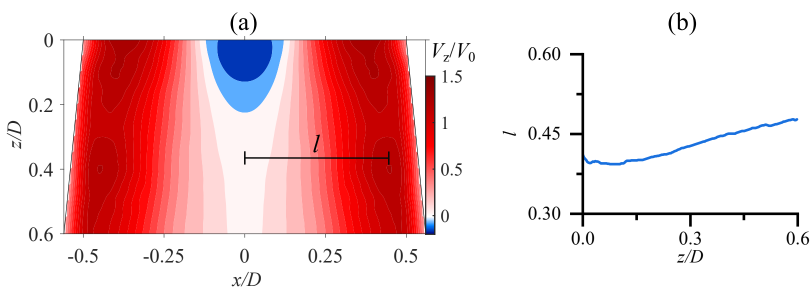

Figure 2. (a): Mean axial velocity field with black line segment. This segment marks the distance l between the minimum and the maximum of the mean axial velocity. (b): The measured distance l as function of axial coordinate z/D.

In this work, the stability problem (7) is solved in the local formulation. Then, the global stability properties of the flow are concluded from the local properties. To conduct a local stability analysis to a turbulent shear flow, several assumptions are made. Firstly, we apply the stability analysis to the mean field, which is not the base flow (the steady solution of the Navier-Stokes equations). It means the analysis is quasi-linear, as it still captures those non-linearities that modify the mean flow. In several previous papers, the adequacy of this approach is shown [15, 16]. Secondly, we assume the mean flow to be perfectly symmetric with respect to the jet axis and only weakly non-parallel in the streamwise direction. This allows for a one-dimensional (local) perturbation Ansatz with a radially dependent amplitude function with periodic azimuthal and axial dependency. Those assumptions are acceptable for prediction of the PVC in swirl flows, as was shown in [6, 7, 17]. According to the mentioned studies, we assume that the radial component of velocity is neglected, to satisfy the continuity equation. Then perturbation Ansatz reads as follows

$$\tilde{\mathbf{q}}(\mathbf{x}, t) \propto \hat{\mathbf{q}}(\mathbf{x}, t) e^{i(\alpha z + m\theta - \omega t)} + c.c, \tag{10}$$

where α is the complex streamwise wave number, ω is the complex frequency, and m is the azimuthal wave number. Here, we present LSA results for the azimuthal wave numbers $m = 0{-}5$.

In this work, the concept of convective and absolute instability connects the local and global stability [18]. The convective instability is determined for each steamwise positions with using of spatio-temporal analysis for the ω and complex α. For this purpose, a special numerical procedure has found the saddle point in the α plane by minimizing the functional $(\partial\omega_i/\partial\alpha_r)^2 + (\partial\omega_i/\partial\alpha_i)^2$ (for more details [7]). The saddle point characterized by complex frequency is called the absolute frequency $\omega_0 = \omega_{0,i} + i\omega_{0,r}$. In this case, the positive values ($\omega_{0,i} > 0$) refer to absolutely unstable flow and the negative values ($\omega_{0,i} < 0$) refer to absolutely stable.

3. Results

3.1. Pressure pulsations

We start the analysis with the evaluation of the level of dominant peaks obtained from PSD pressure spectra (Figure 3) of the decomposed pressure pulsation signals as a function of Q for two azimuthal wave numbers ($m = 1$ and $m = 2$) from [8]. The highest level of pressure fluctuations ($m = 1$) is observed for the flow rate with $0.5Q_c$, as was previously reported in [9]. The curve of the amplitude in the $m = 2$ spectra looks similar to the $m = 1$. The level of $m = 2$ is 80% of the level of $m = 1$ at the flow rate $0.55Q_c$. Thus, the maximal values of the $m = 2$ peak have a too high level to consider it as a higher harmonic of $m = 1$.

Also, the dominant frequencies of $m = 1$ and $m = 2$ spectra are shown as a function of Q/Q_c. The curves have minimum values for the flow regime at $0.5Q_c$. It is noted the $m = 2$ frequency is near the doubled frequency of the $m = 1$ pressure pulsations.

3.2. Stochastic modeling

We proceed the analysis with the stochastic modeling (SM) approach. The purpose of the model is to accurately characterize the bifurcation point, i.e. the point where the flow becomes unstable. According to the theory, the bifurcation point is represented by a zero value of σ. Hence, we apply the SM approach to data at $0.6 - 0.8Q_c$ flow rates, where the PVC appears in the swirl flow (Figure 3).

The analytical model is fitted to the measured $|A|$ PDF function based on the pressure fluctuation signals (see section 2.2). This is done for different flow rates Q/Q_c and, consequently, for the different swirl numbers S. The parameter of the swirl number S is calculated with using of the axial and tangential component of the mean velocity, according to [8].

The form of $|A|$ PDF for the different flow rates is shown in Figure 4a. The PDF starts with broad amplitude distributions on the left side of the plot and then decreases to the narrow low

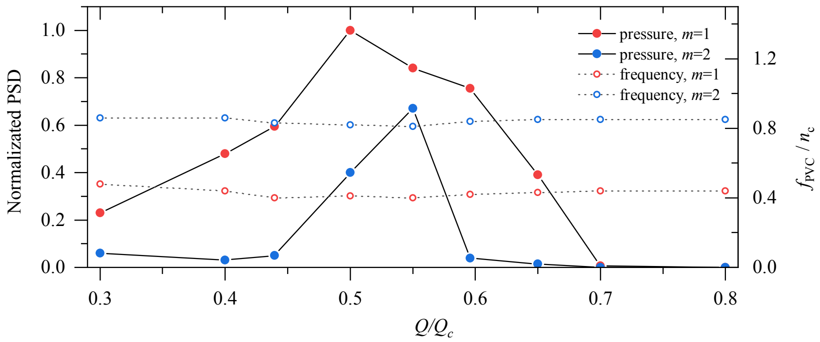

Figure 3. Evolution of maximal pressure fluctuations of $m = 1$ and $m = 2$ as function of the flow rate Q/Q_c. The right axis represents the corresponding PVC frequency.

amplitude distribution on the right side of the plot. Figure 4b shows the SM approximation, which is in good agreement with experimental data. The amplification rate σ predicted by the

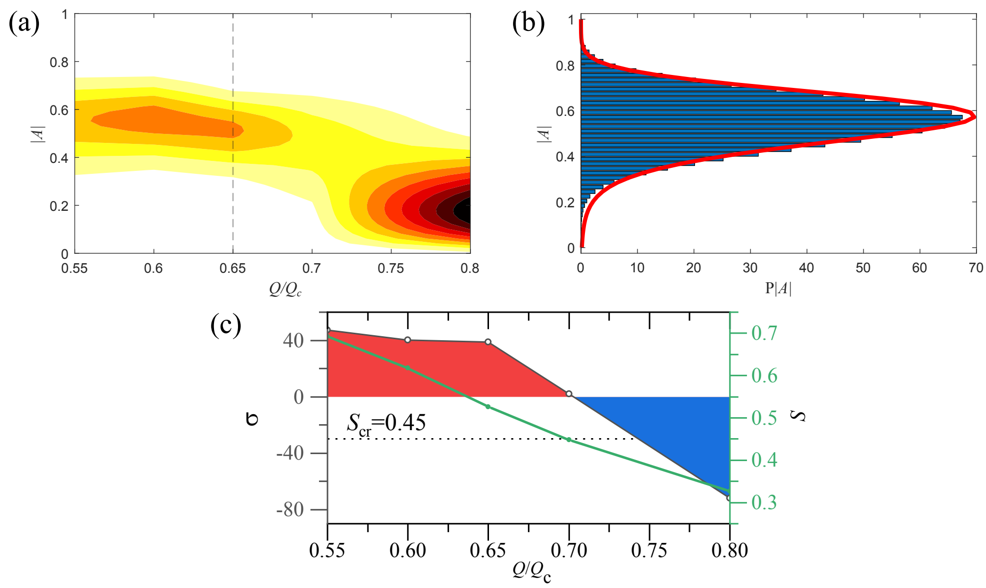

Figure 4. Results of SM: the probability density for different flow rates Q/Q_c (a) and the probability density of $|A|$ at $0.65Q_c$ together with the analytical fit (b) (the regime of Q/Q_c corresponds to the dash line on the plot (a)), and (c) the temporal growth rate σ as function of the flow rate Q/Q_c and swirl number S.

stochastic model as a function of flow rate Q/Q_c is shown in Figure 4c. The right axis represents the swirl number S as the function of flow rate Q/Q_c. The stochastic model predicts the critical flow rate $Q_{cr} = 0.7Q_c$ ($S_{cr} = 0.45$) as the onset of the PVC.

3.3. LSA results
In the beginning, the LSA has been applied to the velocity distribution at the regimes with maximal pressure fluctuation caused by the PVC effect (Figure 3, $0.5Q_c$). The values of $\omega_{0,i}$

and $\omega_{0,r}$ obtained by the local LSA are shown in Figure 5 for the azimuthal wave numbers ranging from $m = 0$ to $m = 5$ at the flow rate $0.5Q_c$. According to the performed analysis (Figure 5a), modes $m = 1$ and $m = 2$ are considered as absolutely unstable, while the azimuthal modes $m = 0, 3, 4, 5$ are absolutely stable everywhere. The mode $m = 1$ corresponds to a single-helical instability [6, 19]. In this work, we report for the first time about the observation of the instability of the mode $m = 2$ in the swirl flow of hydro turbines.

The value of $\omega_{0,r}$ is shown in Figure 5b. The mode $m = 1$ has a relatively good match with the measured non-dimensional PVC frequency (marked by the horizontal red dashed line). Also, the mode $m = 2$ has the same match with the doubled measured non-dimensional PVC frequency. In order to verify the turbulence model included in the linearized equations, computations are

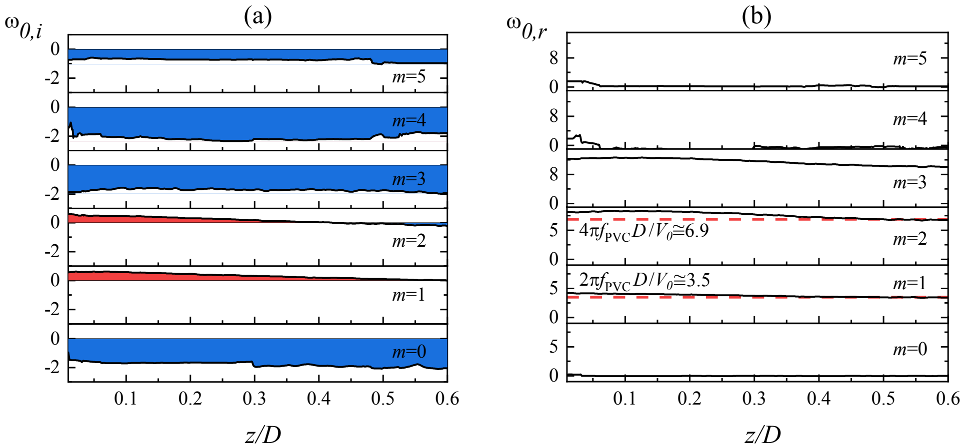

Figure 5. Absolute growth rate (a) and frequency (b) for flow rate $0.5Q_c$ and the azimuthal modes $m = 0$ to 5. Filling area under the curve by red and blue colour means $\omega_{0,i} > 0$ and $\omega_{0,i} < 0$, respectively.

carried out for a quasi-laminar conditions with different Reynolds number Re ranging from 50 to 500 and based on the eddy viscosity model with $Re = \frac{DV_0}{\nu+\nu_t}$ (ν_t from (9)) at the same regime with $0.5Q_c$. The results in terms of $\omega_{0,i}$ and $\omega_{0,r}$ as a function of streamwise direction z/D is shown in Figure 6. The absolute growth rate $\omega_{0,i}$ has a maximum at the inlet of the cone and then slightly decreases with downstream distance. Considering Re=100 and higher, absolute instability exists for the entire streamwise distance (for the $m = 1$ mode). The same result is obtained for the absolute growth rate $\omega_{0,i}$, when based on the eddy viscosity model (9).

The eddy viscosity has major impact on the growth rate $\omega_{0,i}$, but not on the frequency $\omega_{0,r}$, which is typically observed [7]. It should be noted that frequency prediction is in the right range, but for the exact prediction one would need to identify the wave maker, which would require an analytic expansion of the absolute frequency to complex values of z/D [20]. However, an accurate prediction of the PVC frequency is not the focus of this paper.

Finally, we present the absolute growth rate $\omega_{0,i}$, obtained by the local LSA, as a function of the operating condition of the hydro turbine model for two modes, $m = 1$ and $m = 2$ (Figure 7). It is shown that mode $m = 1$ is absolutely unstable starting from $0.3Q_c$ and ending at a flow rate of $0.7Q_c$. Again, the growth rate ω_i has a maximum value at the inlet and then decreases with downstream distance. It is seen that the maximum value of $\omega_{0,i}$ moves downstream (0.6 to $0.65Q_c$). At a flow rate of $0.8Q_c$, the flow becomes stable everywhere, except for a small area of positive growth rate at the upstream location. Considering the stochastic model (Figure 4c), this region does not seem to be sufficiently large to cause the PVC.

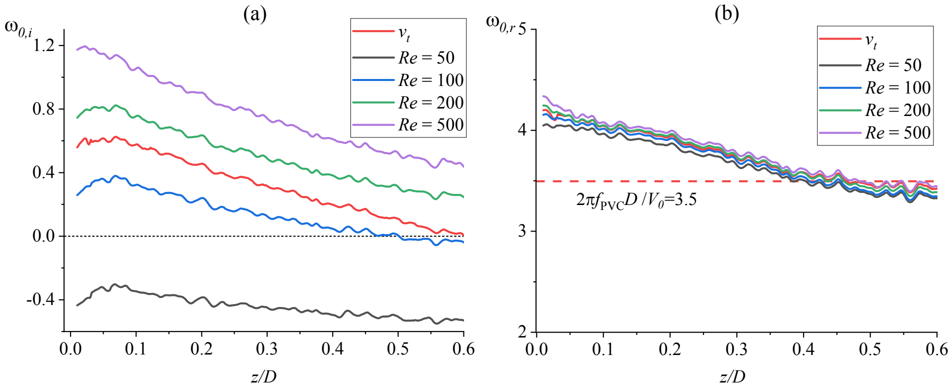

Figure 6. Absolute growth rate $\omega_{0,i}$ (a) and frequency $\omega_{0,r}$ (b) derived from the local LSA for flow rate $0.5Q_c$ and different Re numbers.

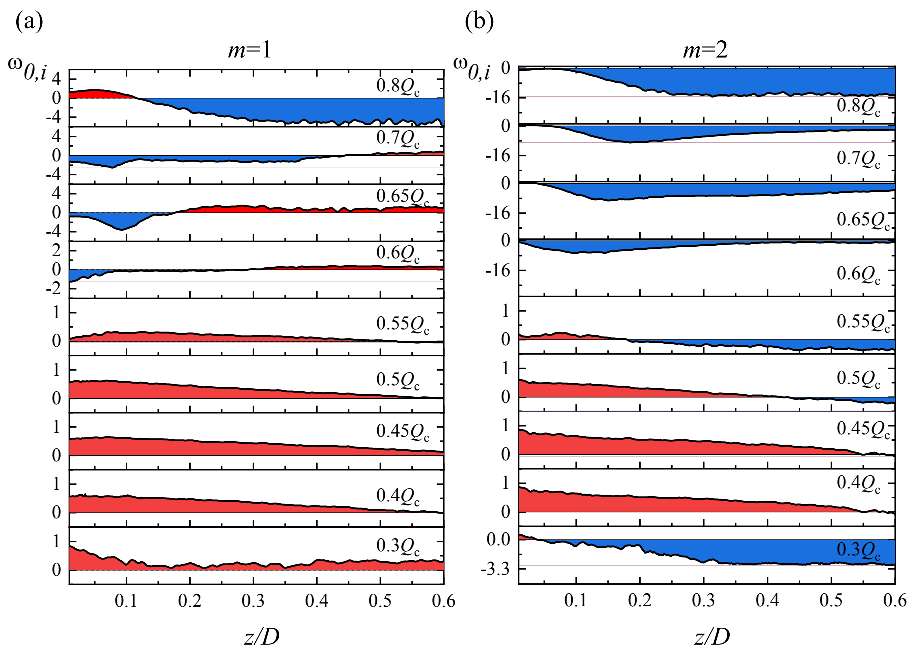

Figure 7. Absolute growth rate $\omega_{0,i}$ for the different flow rates Q/Q_c: (a) for mode $m = 1$, and (b) for mode $m = 2$. Filling area under the curve by red and blue colour means $\omega_{0,i} > 0$ and $\omega_{0,i} < 0$, respectively.

As for the $m = 2$ mode (Figure 7b), it is absolutely unstable for the flow rates, ranging from $0.4Q_c$ to $0.55Q_c$. This is a new observation of instability in the part load regimes of hydro turbines. It provides new insight on the results presented in Figure 3, where the contribution of mode $m = 2$ to the energy content is quite high in the part load regimes (0.5 to $0.55Q_c$) [8]. According to this analysis, the $m = 1$ and $m = 2$ pulsations observed in the pressure spectra are both the consequence of an absolute instability, and due to their harmonic frequency relation (Figure 5) they may easily synchronize to form one coherent structure, which manifests in a PVC.

4. Conclusions

We employ two analytical methods to reveal the root of the PVC dynamics in the hydro turbine model operated over a wide range of flow regimes. Both methods are based on experimental data. The results strongly indicate that the PVC is the primary hydrodynamic instability in the part load regimes of the hydro turbine model.

Firstly, the stochastic modeling approach is used to predict the linear growth rate of the PVC based on time-resolved wall pressure recordings. The stochastic model predicts the growth rates to be positive for the flow rates below $0.7Q_c$. It also predicts the critical flow rate $Q_{cr} = 0.7Q_c$ ($S_{cr} = 0.45$) for the onset of the PVC.

Secondly, local linear stability analysis is employed to the mean fields deduced from PIV measurements. The analysis shows that the flow at the flow rates below $0.7Q_c$ becomes absolutely unstable to modes with azimuthal wave number $m = 1$ and, quite surprisingly, also to the $m = 2$ mode. This is the first observation in the literature that the mode $m = 2$ is absolute unstable in the part load regimes of hydro turbines. Quite interestingly, the frequency of the $m = 2$ mode is double the frequency of the $m = 1$, which implies that these modes are well-aligned to synchronize via their harmonics. The synchronized state of these two modes represents the PVC dynamics.

Acknowledgments

This investigation is supported by the Russian Foundation for Basic Research (project no. 20-58-12012, in the part of PIV measurements). I. Litvinov acknowledges the financial support from the DAAD and the Ministry of Education and Science of the RF (in the part of LSA results) and the Grant for young scientists (project no. MK-1504.2021.4, in the part of the pressure measurements used for the SM approach). The funding of the German Research Foundation (grant number 429772199) is acknowledged.

References

[1] Liang H and Maxworthy T 2005 *Journal of fluid mechanics* **525** 115–159
[2] Syred N 2006 *Progress in Energy and Combustion Science* **32** 93–161
[3] Goyal R and Gandhi B K 2018 *Renewable Energy* **116** 697–709
[4] Sieber M, Paschereit C O and Oberleithner K 2021 *International Journal of Heat and Fluid Flow* **90** 108820
[5] Sieber M, Paschereit C O and Oberleithner K 2021 *Journal of Fluid Mechanics* **916** A7
[6] Oberleithner K, Sieber M, Nayeri C N, Paschereit C O, Petz C, Hege H C, Noack B R and Wygnanski I 2011 *Journal of fluid mechanics* **679** 383–414
[7] Oberleithner K, Stöhr M, Im S H, Arndt C M and Steinberg A M 2015 *Combustion and Flame* **162** 3100–3114
[8] Litvinov I, Sharaborin D, Gorelikov E, Dulin V, Shtork S, Alekseenko S and Oberleithner K 2022 *Applied Science* **12** 5127
[9] Litvinov I, Shtork S, Gorelikov E, Mitryakov A and Hanjalic K 2018 *Experimental Thermal and Fluid Science* **91** 410–422
[10] Sonin V, Ustimenko A, Kuibin P, Litvinov I and Shtork S 2016 *IOP Conf. Ser.: Earth Environ. Sci.* **49** 082020
[11] Reynolds W and Hussain A 1972 *Journal of Fluid Mechanics* **54** 263–288
[12] Rukes L, Paschereit C O and Oberleithner K 2016 *European Journal of Mechanics-B/Fluids* **59** 205–218
[13] Pope S B 2000 *Turbulent Flows* (Cambridge University Press)
[14] Kuethe A M 1935 *Journal of Applied Mechanics* **2** A87–A95
[15] Barkley D 2006 *EPL (Europhysics Letters)* **75** 750
[16] Mantič-Lugo V, Arratia C and Gallaire F 2015 *Physics of Fluids* **27** 074103
[17] Terhaar S, Oberleithner K and Paschereit C O 2015 *Proceedings of the Combustion Institute* **35** 3347–3354
[18] Huerre P and Monkewitz P A 1990 *Annual review of fluid mechanics* **22** 473–537
[19] Pasche S, Avellan F and Gallaire F 2017 *Journal of fluids engineering* **139** 4051102
[20] Chomaz J M 2005 *Annu. Rev. Fluid Mech.* **37** 357–392